JOURNAL OF GEOPHYSICAL RESEARCH, VOL. 98, NO. D4, PAGES 7165–7180, APRIL 20, 1993

Global NO_x, HNO_3, PAN, and NO_y Distributions From Fossil Fuel Combustion Emissions: A Model Study

P. S. KASIBHATLA[1]

School of Earth and Atmospheric Sciences, Georgia Institute of Technology, Atlanta

H. LEVY II AND W. J. MOXIM

Geophysical Fluid Dynamics Laboratory, Princeton University, Princeton, New Jersey

The 11-level Geophysical Fluid Dynamics Laboratory global chemical transport model (GCTM) which explicitly treats NO_x, HNO_3, and PAN as transported species has been used to assess the impact of fossil fuel combustion emissions on the distribution of reactive nitrogen compounds (NO_y) in various regions of the troposphere. The GCTM is driven by 6-hour time-averaged wind and total precipitation fields derived from a parent general circulation model. PAN production rates are calculated using background, two-dimensional ethane and propane fields, which are then adjusted to parameterize the effect of short-lived hydrocarbons over continental regions. From an analysis of our model results, we conclude that (1) the model reproduces the observed spatial patterns of wet deposition near the major fossil fuel combustion source regions. Wet and dry deposition in source regions account for 30% and 40–45% of the emissions, respectively, with the remainder being exported over the adjacent ocean basins; (2) the fossil fuel source accounts for a large fraction of the observed surface concentrations and wet deposition fluxes of HNO_3 in the extra tropical North Atlantic; (3) while it appears that a significant fraction of NO_y observed in the marine free troposphere during the NASA Global Tropical Experiment/CITE 2 experiment in the eastern North Pacific cannot be explained in terms of the fossil fuel source, this may simply indicate that in this region subgrid-scale transport from adjacent continental source regions is not being adequately resolved by the model; (4) at the more remote Mauna Loa, Hawaii site, less than 30% of the observed NO_y during May 1988, appears to be due to distant fossil fuel sources; (5) even with the explicit treatment of PAN as a transported species, the fossil fuel source has only a minor impact on NO_y levels in the remote tropics and in the southern hemisphere; (5) model calculations indicate that the relatively high levels of NO_y observed over western Alaska during the ABLE 3A experiment in July–August 1988, cannot be explained in terms of long-range transport of fossil fuel combustion emissions from the northern hemisphere mid-latitude surface source regions; and (6) away from source regions, PAN is a major component of fossil fuel NO_y, and is the dominant component poleward of 45°N. However, the relative impact of this sequestered PAN on regional spring time NO_x levels has yet to be established.

INTRODUCTION

The ubiquitous role of NO_x (NO + NO_2) in determining the global oxidizing power of the troposphere has long been recognized [*Levy*, 1971; *Crutzen*, 1974]. A comprehensive understanding of the factors controlling the spatial and temporal distribution of NO_x is therefore important in establishing the influence of humans on atmospheric chemistry in particular, and on global climate in general. From a broader perspective, it is also important to understand the processes controlling the biogeochemical cycling of reactive nitrogen compounds (NO_y). In recent years, considerable advances in our understanding of the atmospheric component of the NO_y cycle have resulted from a combination of field and laboratory studies. In addition, three-dimensional global chemical transport models have steadily evolved to provide us with a tool with which to synthesize the information gathered from these field and laboratory studies. Nevertheless, significant gaps exist in our knowledge of the global atmospheric NO_y budget. At present, it is generally accepted that the major tropospheric NO_y sources are fossil fuel combustion, biomass burning, biogenic emissions from soils, and lightning discharges, with a small contribution from downward transport of NO_x produced by N_2O oxidation in the stratosphere [*Logan*, 1983]. In addition, emissions from aircraft may have a significant impact on upper tropospheric NO_x levels in northern hemisphere (NH) mid-latitudes [*Beck et al.*, 1992].

This paper is the second in a series of papers aimed at quantifying the magnitude of the individual sources of NO_x, as well as the spatial distribution and temporal variation of the individual reactive nitrogen compounds resulting from these sources. An earlier paper [*Kasibhatla et al.*, 1991] focused on the impact of the stratospheric photochemical source. A key conclusion from that study was that the stratospheric source was unable to account for more than a very small fraction of observed background surface NO_y concentrations, which is in accord with similar conclusions by *Logan* [1983] and *Penner et al.* [1991]. Similarly, a comparison with the limited number of observations in the remote mid- and upper troposphere revealed that substantial

[1]Visiting Scientist at Geophysical Fluid Dynamics Laboratory, Princeton University, Princeton, New Jersey.

Paper number 92JD02845.
0148-0227/93/92JD-02845$05.00

contributions from other NO_y sources were needed to explain those observations.

This paper focuses on the distribution of reactive nitrogen compounds resulting from fossil fuel combustion emissions alone. This source, located mainly in the NH mid-latitudes, is estimated to be ~21 Tg N/yr. *Levy and Moxim* [1989*a*] used the same transport model as the one used in this study to estimate the global impact of this fossil fuel source. This study, however, differs significantly from that by *Levy and Moxim* [1989*a*] in that they treated the collection of reactive nitrogen compounds as a single species, namely, NO_y. A practical difficulty with such an approach arises when calculating effective dry and wet removal rates for NO_y as its chemical partitioning changes, since different component species of NO_y have different wet and dry removal rates. In this study, we explicitly treat NO_x, HNO_3, and peroxyacetyl nitrate (PAN) as transported species and use an off-line chemical scheme to calculate the interconversion rates among these species. In effect, we are using NO_x, HNO_3, and PAN as surrogates for insoluble inorganic, soluble inorganic, and reservoir organic NO_y species, respectively. This approach also enables us to compare our model results with observations of both NO_y and its major components. In this context it should be mentioned that measured concentrations of NO_y often exceed the sum of the measured concentrations of NO_x, HNO_3 (and particulate nitrate), and PAN (and organic nitrates), sometimes by as much as 25–50% [e.g., *Ridley*, 1991; *Atlas et al.*, 1992; *Jacob et al.*, 1992]. In these regions, where some "missing" component makes up a significant fraction of the total NO_y, it may be more appropriate to interpret the model results in terms of the total NO_y rather than in terms of the individual NO_y components.

It should also be noted here that *Penner et al.* [1991] have used a three-dimensional Lagrangian transport model to study the global distribution of reactive nitrogen compounds. Our study differs from theirs in two significant respects: (1) The calculations by *Penner et al.* [1991] partition NO_y into NO_x and HNO_3, while we explicitly treat PAN as a transported species, thus providing an insoluble organic reservoir for NO_y; and (2) the simulations by *Penner et al.* [1991] are for perpetual January and July conditions, whereas our calculations are for the entire annual cycle.

Section 2 provides an overview of the GCTM. The design of the numerical experiments is described in section 3, and the results from these experiments are presented and compared with available observations in section 4. Our conclusions are summarized in section 5.

2. Brief Description of the Model

The global chemical transport model (GCTM) in this study has a horizontal resolution of ~265 km, and 11 vertical levels at standard pressures of 990, 940, 835, 685, 500, 315, 190, 110, 65, 38, and 10 mbar. The model is driven by 12 months of 6-hour time-averaged wind and total precipitation fields derived from a parent general circulation model (GCM) [*Manabe et al.*, 1974; *Manabe and Holloway*, 1975]. The meteorological features of the GCM have been the subject of many previous studies, and the interested reader may wish to refer to the paper by *Mahlman and Moxim* [1978] for a comprehensive list of references pertaining to the GCM.

The basic structure of the GCTM and calculation of flux divergences has been described by *Mahlman and Moxim* [1978]. The GCTM incorporates parameterized horizontal subgrid scale transport, as well as vertical mixing by dry and moist convection. Complete descriptions of these parameterizations are given by *Levy et al.* [1982, Appendix A]. In the standard formulation of the model [*Levy et al.*, 1982], vertical turbulent mixing occurs only when the atmosphere is convectively unstable (dry or moist). *Levy and Moxim* [1989*a*] found that under conditions of large-scale stability, the model underestimated mixing in the boundary layer. They therefore modified the formulation to include an additional shear-dependent vertical diffusion (which is independent of the large-scale stability) in the bottom three model levels. The form of this additional term is

$$K_{vbl} = A[L(z)]^2 \left| \frac{\partial}{\partial z} \bar{V} \right|, \tag{1}$$

where, $L(z)$ is the height-dependent mixing length used by the parent GCM, and $(\partial/\partial z)\ \bar{V}$ is the vertical wind shear. While *Levy and Moxim* [1989*a*] used a value of $A = 0.1$ in their study, we find that this value overestimates the NO_y gradient between the model 990 and 940-mbar model levels relative to a limited set of aircraft profiles [*Van Valin et al.*, 1991]. In the current study, we use a value of $A = 0.5$, thereby enhancing vertical mixing in the model boundary layer and reducing the gradient between the 990 and 940-mbar model levels.

Dry deposition is calculated based on the assumption of a balance between surface deposition and the turbulent flux in the bottom half of the lowest model level. This assumption enables one to calculate the tracer dry deposition tendency as

$$\frac{\partial}{\partial t} R_{11}(i)\Big|_{\text{dry}} = \frac{w_d(i)}{\Delta z} \left\{ \left[(R_{11}(i)) \frac{1}{[1 + w_d(i)/(C_d|\bar{V}_{\text{eff}}|)]} \right] \right\}, \tag{2}$$

where, $R_{11}(i)$ is the mixing ratio of species i in the lowest model level, $w_d(i)$ is its deposition velocity, Δz is the thickness of the bottom model level, C_d is the GCM's globally averaged surface drag coefficient (0.002), and $|\bar{V}_{\text{eff}}|$ is the model's effective surface wind speed (see *Levy and Moxim* [1989*a*, section 2.4] for details). The wet removal scheme used to simulate precipitation scavenging of HNO_3 distinguishes between stable or shallow convective and deep convective precipitation. The fraction of tracer removed from a model grid box is a function of the local precipitation rate, and the wet removal tendency is proportional to the local tracer mixing ratio (see *Kasibhatla et al.* [1991, section 2] for details).

The chemical production and loss rates of the three transported species (NO_x, HNO_3, and PAN) are calculated off-line, using a standard O_3-CO-CH_4-NO_x-H_xO_y chemical scheme [e.g., *Chameides and Tan*, 1981] and are carried in the GCTM as temporally varying, two-dimensional fields. The nighttime conversion of NO_x to HNO_3, by the reaction of NO_2 with O_3, followed by the reaction of NO_3 with NO_2, is included in the bottom two model levels. The rate at which this conversion occurs is limited by the total aerosol surface area per unit volume, and a detailed analysis of summer time data from a rural site in the eastern United States suggests that this process is significant only in the bottom kilometer or

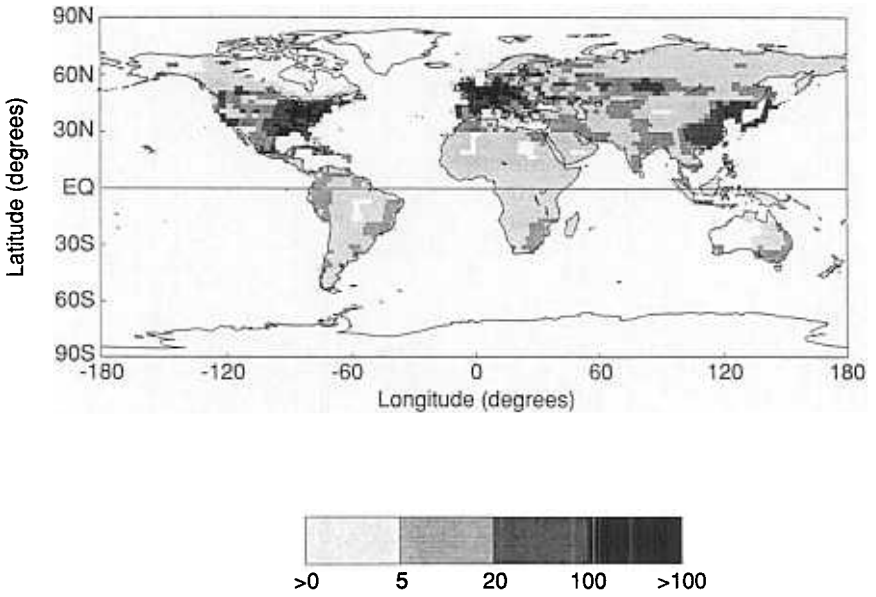

Fig. 1. Annual fossil fuel combustion reactive nitrogen source (mmoles N m^{-2} yr^{-1}).

or so [*Trainer et al.*, 1991]. Kinetic parameters for most reactions are specified according to *DeMore et al.* [1990]. Rate expressions recommended by *Atkinson and Lloyd* [1984] are used for the reaction of the peroxyacetyl radical with NO and NO_2, and for the thermal decomposition of PAN, while the PAN + OH reaction rate is specified according to *Singh et al.* [1992]. The CH_4 + OH reaction rate has been updated according to *Vaghjiani and Ravishankara* [1991].

Inputs to the off-line chemical calculation include hemispherically averaged one-dimensional CO and NO_x profiles and two-dimensional fields of CH_4, O_3, H_2O, temperature, and total column ozone. These fields are specified either from available observations or GCM data (see *Kasibhatla et al.* [1991, appendix] for details). In our model, PAN formation occurs via the reaction of peroxyacetyl radical (PAC) with NO_2. The PAC, in turn, is generated by the reaction of nonmethane hydrocarbons (NMHCs) with OH (see *Kasibhatla et al.* [1991, section 3] for details). NMHC concentrations used to calculate PAN formation rates are specified according to model-calculated, two-dimensional, monthly varying ethane and propane fields from *Kanakidou et al.* [1991]. Over continents, short-lived natural hydrocarbons, such as isoprene, can contribute significantly to PAN formation [e.g., *Trainer et al.*, 1991]. In order to take this into account, we have adjusted NMHC levels so as to approximately reproduce observed summer time PAN levels at a rural site in the eastern United States (Scotia, Pennsylvania), as well as PAN fractions measured during periods of east winds at Boulder in February (M. P. Buhr, private communication, 1992), and at Egbert, Ontario in April [*Shepson et al.*, 1991]. To accomplish this, we have increased NMHC concentrations over land in the bottom three model levels between 30°N and 65°N by a factor of 3 in summer, and by a factor of 1.5 in spring and fall, relative to the two-dimensional fields of *Kanakidou et al.* [1991]. South of 30°N, NMHC concentrations over land in the bottom three model levels have been adjusted so that, throughout the year, they are approximately equal to summer time, lower tropospheric NMHC concentrations over land specified between 30°N and 65°N. The rationale for this stems from studies [e.g., *Chameides et al.*, 1992] which find that, on an OH reactivity-based scale, surface hydrocarbon levels observed over remote tropical forests are comparable to those in the rural areas of the eastern United States during summer.

We feel that our approach of treating PAN chemistry in a global, three-dimensional transport model offers a reasonable compromise between approaches which neglect PAN chemistry entirely in three-dimensional model simulations [e.g., *Penner et al.*, 1991] and approaches which treat PAN chemistry more comprehensively, albeit in a two-dimensional transport model framework [e.g., *Kanakidou et al.*, 1991].

3. Design of the Experiments

The construction of the gridded fossil fuel source data base for NO_x uses detailed emission inventories from the United States, Canada, and Europe, supplemented with global estimates by *Hameed and Dignon* [1988] that are based on United Nations fuel use statistics (for details see *Levy and Moxim* [1989*a*]). We have added 0.015 Tg N yr^{-1} of NO_x emissions from Prudhoe Bay [*Jaffe et al.*, 1991] for this study. However, emissions from commercial aircraft (~0.5 Tg N yr^{-1}) are not included in the current study. While much smaller than the other fossil fuel combustion sources, this direct emission into the free troposphere may have a significant impact on NO_x mixing ratios in the upper troposphere [*Beck et al.*, 1992]. The annual source strength is 21.3 Tg N yr^{-1}, with North America and Europe accounting for 7.5 and 5.9 Tg N yr^{-1}, respectively. The geographical distribution of the emissions is shown in Figure 1. In the GCTM, the emissions at each location are partitioned into a surface flux, and volume sources in the bottom two model levels in the manner described by *Levy and Moxim* [1989*a*].

Dry deposition velocities used in the model reflect measured deposition velocities of individual reactive nitrogen species [*Cadle et al.*, 1985; *Huebert and Robert*, 1985;

Wesely et al., 1982; *Walcek et al.*, 1986; *Voldner et al.*, 1986]. The dry deposition velocities of NO_x and PAN are assumed to be 0.0 over oceans, ice, and snow. Over ice and snow, the HNO_3 dry deposition velocity is assumed to be 0.5 cm s^{-1}. Over oceans, where particulate nitrate may be an important component of the inorganic soluble nitrogen, a dry deposition velocity (w_d) of 0.3 cm s^{-1} is used for HNO_3 [*Prospero et al.*, 1990]. Over land, when the temperature in the lowest model level (T_{11}) is greater than 10°C, w_d is 1.5 cm s^{-1} for HNO_3, and 0.25 cm s^{-1} for NO_x and PAN. The case when $T_{11} < -10$°C is treated the same as ice and snow. For temperatures between −10°C and 10°C over land, the w_d values are linearly interpolated between the two land values mentioned above (H. Levy et al., unpublished manuscript, 1992).

In subsequent discussions we will refer primarily to results from two model experiments. The first experiment will be referred to as the STDWET experiment, and model parameters are as defined above. The second experiment is designed to explore the sensitivity of simulated tracer distributions to the rate at which HNO_3 is scavenged by precipitation. The HNO_3 wet removal rates used in the STDWET experiment are 1.2–2 times higher than those calculated using an independent parameterization by *Giorgi and Chameides* [1986] for highly soluble aerosols and gases. For the purposes of this sensitivity study, we have therefore reduced HNO_3 wet removal rates by a factor of 2 in the second model experiment. This experiment will be referred to as the LOWWET experiment. In addition, where appropriate, we will refer to results from a third model experiment, namely, the LOWDRY experiment. This experiment is designed to study whether simulated surface HNO_3 mixing ratios at certain remote sites may be underestimated due to the fact that dry deposition over tropical and subtropical oceans may be overestimated by the model. This, in turn, may be due to an inadequate resolution of the trade wind inversion in the parent GCM. This aspect of our study is further discussed in section 4.3.

A preliminary evaluation of model performance is obtained by comparing model results with summer time surface reactive nitrogen measurements near Scotia, Pennsylvania [*Ridley*, 1991]. Note, however, that lower tropospheric, summer time NMHC levels in the model have been adjusted to approximately reproduce observed surface PAN mixing ratios at this site. The Scotia data set is chosen as a point of comparison partly due to the completeness of the data set in terms of the various NO_y fractions. In addition, the measurements are not directly impacted by local sources and therefore provide a reasonable representation of the regional scale distribution of NO_y in the U.S. source region. Furthermore, Scotia is located in a relatively "clean" model box lying between the polluted western Pennsylvania (and Ohio) and eastern Pennsylvania (and New Jersey) source regions in the GCTM.

Comparisons of simulated and observed surface NO_x, HNO_3, PAN, and NO_y during the summer time at Scotia are presented in Table 1. It may be noted that, while the model reproduces observed surface NO_x mixing ratios, HNO_3 is overpredicted in both model simulations. This is probably due to the fact that the observations are influenced by the efficient removal of HNO_3 from the stable nocturnal boundary layer by dry deposition [*Trainer et al.*, 1991]. The lack of a diurnal cycle in the parent GCM precludes us from simulating this process, resulting in HNO_3 mixing ratios which are significantly higher than the 24-hour average observations.

TABLE 1. Comparison of Simulated July Mean Surface No_x, HNO_3, PAN, and NO_y With Measurements at Scotia, Pennsylvania[a]

	Surface Mixing Ratio, ppbv			
	NO_x	HNO_3	PAN	NO_y
OBS[b]			0.6	
STDWET[c]			0.54	
LOWWET[d]			0.54	

[a]The measurements are provided by the NOAA Aeronomy Laboratory (F. Fehsenfeld, D. Parrish, R. Norton, M. Buhr, G. Hübler, and E. Williams).
[b]NO_x, PAN, and NO_y mixing ratios represent mean mixing ratios measured during July 1986 [*Ridley*, 1991]. HNO_3 is deduced as $HNO_3 = NO_y - NO_x - PAN$.
[c]Model results from the STDWET experiment.
[d]Model results from the LOWWET experiment.

The results of our model calculations are presented in the next section. Simulated global distributions of NO_x, HNO_3, and PAN resulting from fossil fuel combustion emissions are presented in section 4.1, and the sensitivity of these results to model HNO_3 wet removal rates is discussed. Section 4.2 focuses on a comparison of model-simulated wet deposition with observations at specific sites in the North American and European source regions. Simulated wet deposition fluxes and surface concentrations of soluble reactive nitrogen compounds are compared with observations at regional sites in the North Atlantic in section 4.3, while comparisons with surface and mid-tropospheric measurements in the North Pacific are presented in sections 4.4 and 4.5, respectively. Finally, the impact of long-range transport of fossil fuel combustion emissions on NO_y mixing ratios in the remote troposphere, and in the high northern latitudes, is assessed in sections 4.6 and 4.7, respectively.

4. RESULTS OF THE EXPERIMENTS

All simulations were initialized with uniform mixing ratios of 1 pptv of NO_x, HNO_3, and PAN, respectively, and integrated for a period of 18 months from a model start-up date of February 1, until sources and sinks were in balance. In the rest of this paper, we will only discuss results from the last 12 months of each simulation.

4.1. *Global Distributions of NO_x, HNO_3, and PAN*

In this section, we discuss some general features of the simulated global distributions of NO_x, HNO_3, and PAN. We first focus on results from the STDWET experiment, and examine the spatial and temporal characteristics of simulated tracer fields. The sensitivity of our results to the HNO_3 wet removal rate is then assessed by comparing results from this simulation to those from the LOWWET simulation.

January and July mean, surface NO_x, HNO_3, and PAN fields from the STDWET experiment are presented in Figures 2 and 3, respectively. As expected, all three tracers exhibit maxima in the major mid-latitude source regions. Maximum winter time surface mixing ratios range from 2 to >5 parts per billion by volume (ppbv) of NO_x, 2–5 parts per

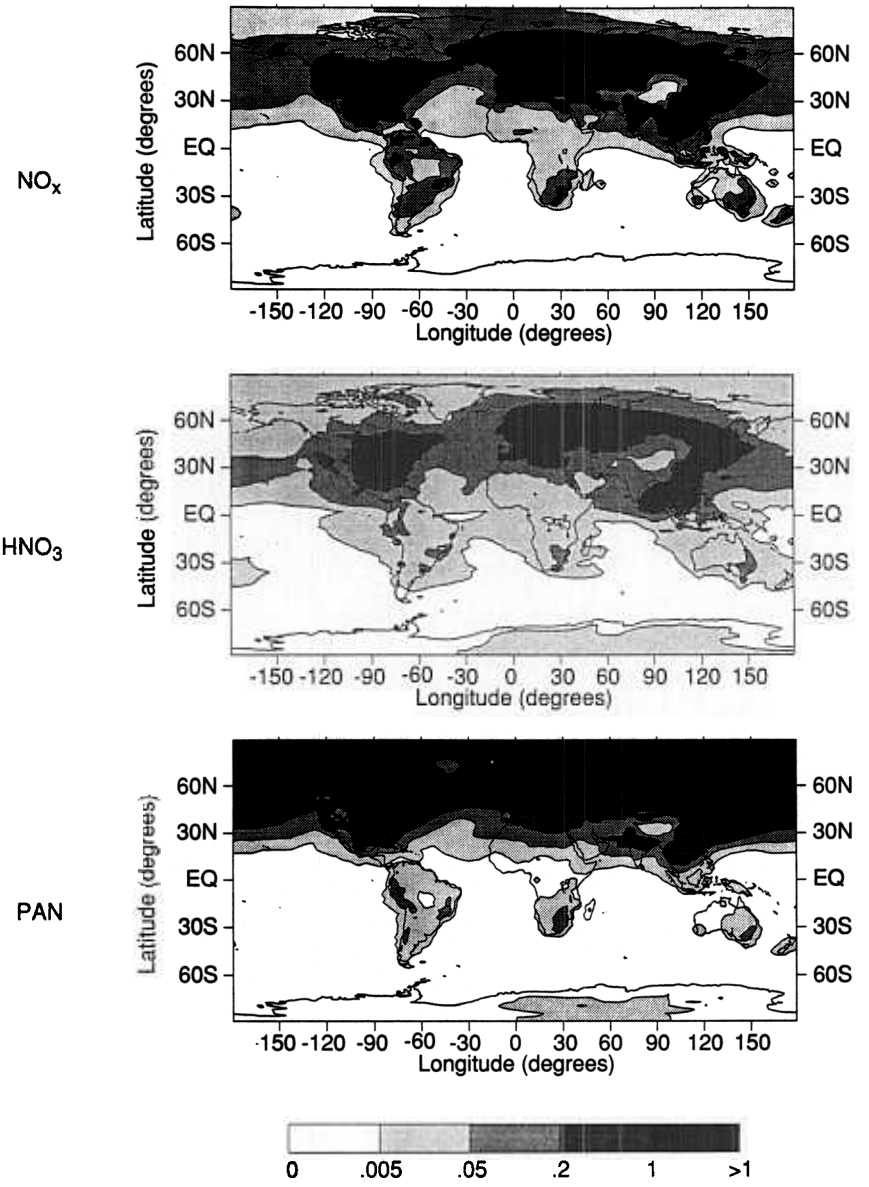

Fig. 2. Simulated January mean surface NO_x, HNO_3, and PAN mixing ratios from the STDWET experiment with the fossil fuel source alone. All values are in ppbv.

billion by volume (ppbv) of HNO_3, and 1–2 ppbv of PAN. Shorter chemical lifetimes and enhanced vertical mixing lead to summer time surface NO_x and PAN levels being approximately a factor of 2 lower than corresponding winter time mixing ratios in source regions. Winter time surface mixing ratios of all three tracers are also higher than summer time levels downwind of major source regions, due to stronger transport and slower photochemistry. Summer time NO_x and PAN, in particular, exhibit strong gradients as one moves from continental source regions to more remote oceanic areas, with mixing ratios rapidly decreasing to below 5 parts per trillion by volume (pptv). Simulated surface NO_x mixing ratios during winter are relatively high (200–500 pptv) along the North Atlantic storm track, and over the western Pacific downwind of the Asian source region (100–200 pptv). PAN is seen to be a major component of fossil fuel NO_y at the surface poleward of 30°N in winter, and even in summer at high northern latitudes. Another distinct feature of the surface maps is the very low level of fossil fuel NO_y over the remote southern hemisphere (SH) oceans, corroborating the conclusion by *Levy and Moxim* [1989*a*] regarding the minimal impact of the predominantly northern hemisphere (NH) fossil fuel source on SH NO_y levels.

Simulated January and July mean NO_x, HNO_3, and PAN distributions at the 500 mbar model level are shown in Figures 4 and 5, respectively. By contrast to the surface distributions, simulated mid-tropospheric distributions are quite zonal, due to stronger transport and slower photochemistry. Poleward of 45°N, simulated NO_x and PAN mixing ratios are relatively high in January, while summer time HNO_3 mixing ratios are significantly higher than winter time values downwind of the major fossil fuel source regions. Once again, our simulations indicate that PAN is a major component of NO_y, particularly in winter. We are currently investigating the specific mechanisms involved in the transport of PAN to the high northern latitude mid-

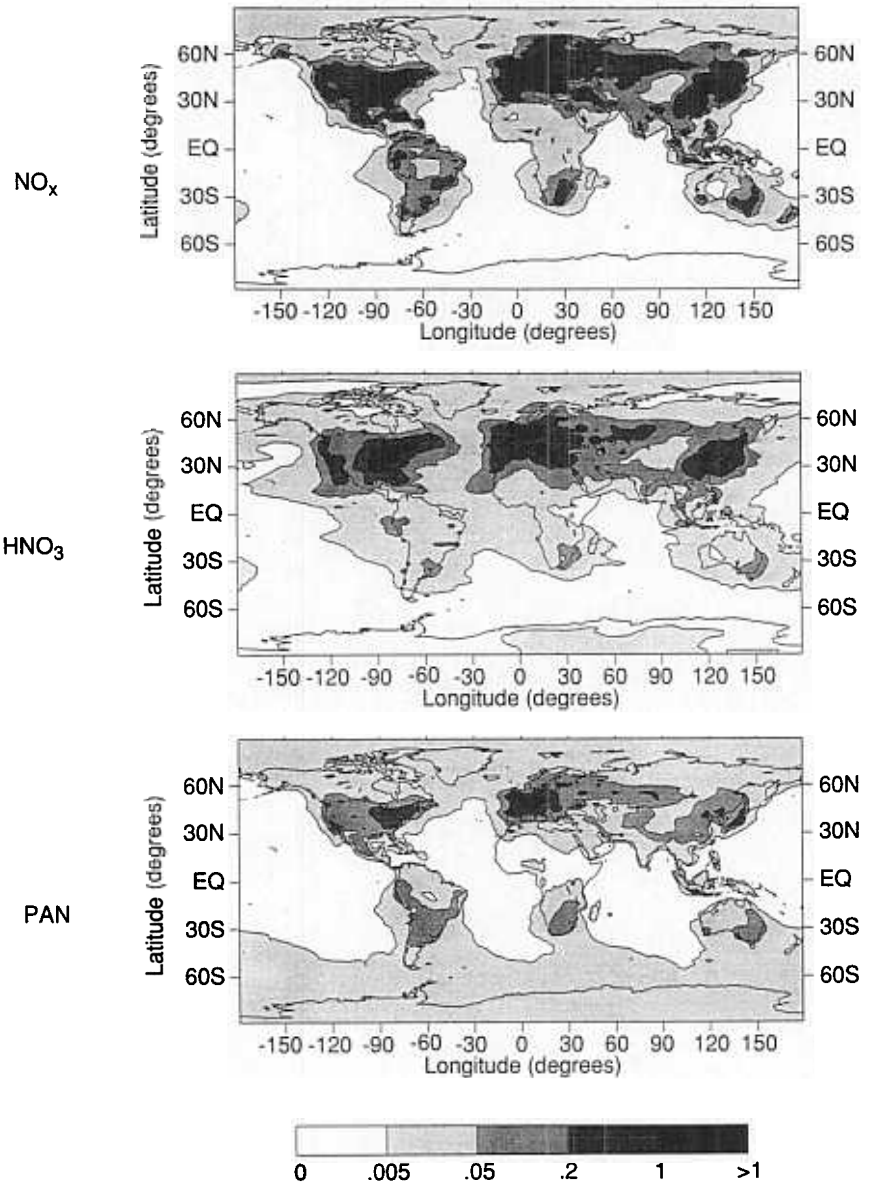

Fig. 3. Simulated July mean surface NO_x, HNO_3, and PAN mixing ratios from the STDWET experiment with the fossil fuel source alone. All values are in ppbv.

troposphere. An additional avenue of current investigation relates to the impact of this sequestered PAN on regional NO_x levels during the transition from winter months to warmer spring months.

Given the fact that our model simulations indicate that PAN is a major component of fossil fuel NO_y at mid- and high northern latitudes, an interesting question is whether neglecting PAN chemistry has a significant effect on the simulated NO_x distribution. To answer this, we have performed an independent simulation in which NO_x and HNO_3 are the only transported species. In general, our results indicate that simulated surface NO_x mixing ratios in source regions are up to 10% higher when PAN chemistry is neglected in the model. In regions which are predominantly affected by transport from source regions (such as along the North Atlantic storm track in winter), this increase in the effective NO_x source leads to a corresponding overestimate of simulated NO_x mixing ratios when PAN chemistry is neglected. In other regions, where a principal source of NO_x is the thermal decomposition of PAN, neglecting PAN chemistry has the effect of underestimating the amount of NO_x present. While it is true that this effect is largely confined to regions where simulated NO_x concentrations are already extremely low, there are locations where this underestimate can be quite significant. For example, if PAN chemistry is neglected, simulated January mean surface mixing ratios of NO_x at 30°N in the central Pacific (50–100 pptv in the STDWET experiment) decrease by a factor of 2–3. Thus neglecting PAN chemistry in the model can have a significant effect on the simulated NO_x distribution.

We next examine the effect of decreasing HNO_3 wet removal rates on simulated tracer distributions from fossil fuel combustion emissions. Over continents, decreasing the wet removal rate has the effect of increasing simulated

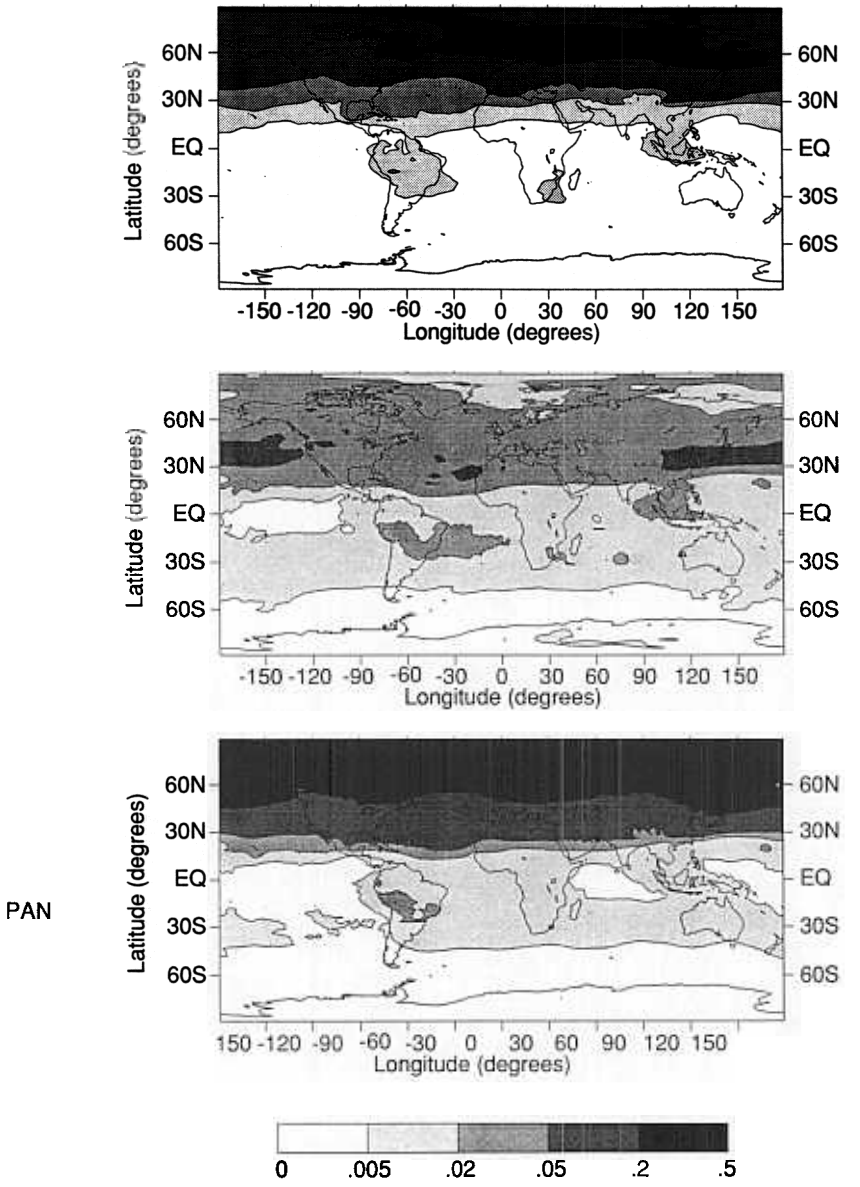

Fig. 4. Simulated January mean 500-mbar NO_x, HNO_3, and PAN mixing ratios from the STDWET experiment with the fossil fuel source alone. All values are in ppbv.

surface HNO_3 mixing ratios by up to a factor of 1.4. Over more remote oceanic regions in the NH, simulated surface HNO_3 concentrations increase by a factor of 1.4–2. Similarly, 500 mbar HNO_3 mixing ratios are about 1.4–1.7 times higher over most regions, with the larger increases seen in the tropical regions where convective wet removal is important. The impact on the simulated NO_x distribution from fossil fuel combustion is confined to the tropics, the subtropics, and the summer hemisphere, in regions where the reaction of HNO_3 with OH is comparable to PAN thermal decomposition as the principal NO_x source. Although NO_x mixing ratios from the LOWWET experiment are 1.4–3 times higher than NO_x mixing ratios from the STDWET experiment, the impact of fossil fuel combustion emissions on NO_x is quite low in these regions.

4.2. *Wet Deposition in Mid-Latitude Source Regions*

The removal of HNO_3 by the physical processes of rainout and washout is an important sink of atmospheric NO_y. An adequate simulation of the wet removal of HNO_3 in source regions is therefore a key ingredient in determining the amount of reactive nitrogen that can be exported from the source regions to more remote regions of the troposphere. In this section we evaluate our current multiple-species model simulation of wet removal by comparing our results with observations of wet deposition fluxes in North America and Europe.

Table 2 shows such a comparison for various U.S. and Canadian sites. Halving the HNO_3 wet removal rate lowers modeled wet deposition fluxes at these sites by 15–30%.

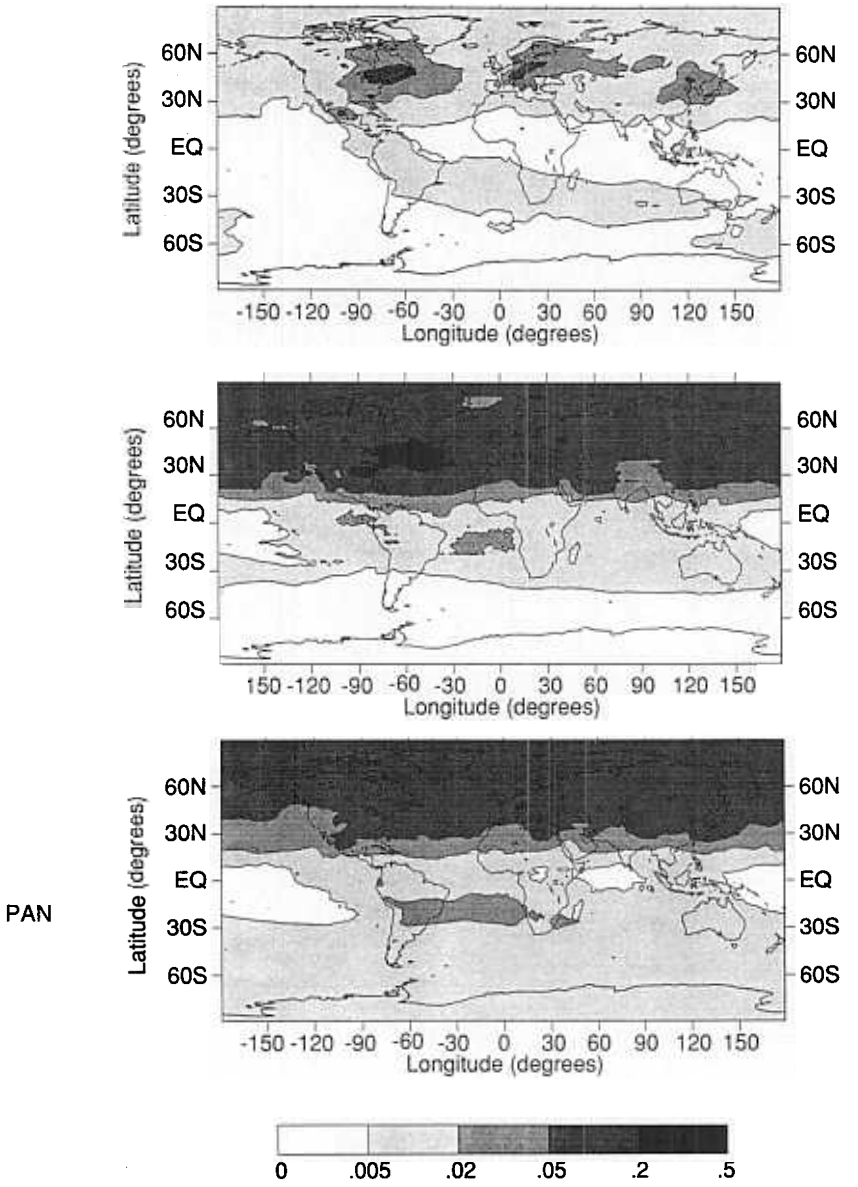

Fig. 5. Simulated July mean 500-mbar NO_x, HNO_3, and PAN mixing ratios from the STDWET experiment with the fossil fuel source alone. All values are in ppbv.

Thus the increase in HNO_3 mixing ratios compensates, to some extent, the decrease in the wet removal rate, leading to a less than proportional decrease in the calculated wet deposition fluxes. Overall, the agreement with the observed deposition fluxes is very good, though there is tendency to overpredict wet deposition fluxes at sites near high-emission regions due to the inability of the model to resolve sharp gradients near strong sources. Table 3 shows a similar comparison for selected sites in Europe. These sites (see *Levy and Moxim* [1989*a*, Figure 5] for the location of the sites) were chosen so as to include sites in the source region itself, as well as sites which are mainly affected by transport from the European source region. The large discrepancy at Hummelfjell, Norway, is due to the fact that the parent GCM significantly underpredicts the precipitation at that site since it does not resolve the topographical features producing the precipitation. In general, the model reproduces the observed spatial patterns in wet deposition fluxes over Europe quite well. The model-calculated yearly wet deposition flux over western Europe (see *Levy and Moxim* [1989*a*, Figure 5] for region boundaries) is 1.3 Tg N yr^{-1} for the LOWWET experiment, and 1.5 Tg N yr^{-1} for the STDWET experiment. This latter value compares well with the observed wet deposition flux of 1.6 Tg N yr^{-1} [*Schaug et al.*, 1987]. While very limited data are available for the Asian source region, model-simulated wet deposition fluxes of 6–12 mMoles N m^{-2} yr^{-1} at Guizhou, China, are in good agreement with measurements of 12 ± 3 mMoles N m^{-2} yr^{-1} [*Galloway et al.*, 1987]. In all three major source regions, about 30% of the emissions undergo wet deposition in the source regions, while dry deposition in the source regions accounts for another 40–45% of the emissions. Thus approximately 25–30% of the emissions are exported from these source regions to the adjacent ocean basins. This estimate agrees well with

TABLE 2. Comparison of Simulated Annual HNO_3 Wet Deposition Fluxes With Observations at Various North American Locations

Location	HNO_3 Wet Deposition Flux, mmoles m^{-2} yr^{-1}		
	OBS[a]	STDWET[b]	LOWWET[c]
Oak Ridge, Tenn.	21	22	17
Oxford, Ohio	24	29	21
Urbana, Il.	22	40	28
Charlottesville, Va.	25	34	26
State College, Pa.	33	36	30
Ithaca, N.Y.	30	44	36
Chalk River, Ontario	24	29	24
Whiteface, N.Y.	21	37	31
Lewes, Del.	22	31	23
Brookhaven, N.Y.	22	33	26
Montmorency, Quebec	25	25	23

[a]Observed annual HNO_3 wet deposition flux [*Dana and Easter*, 1987; *Vet et al.*, 1986].
[b]Simulated annual HNO_3 wet deposition flux from the STDWET experiment.
[c]Simulated annual HNO_3 wet deposition flux from the LOWWET experiment.

a previous estimate by *Logan* [1983] regarding export of North American combustion emissions.

The comparisons of wet deposition fluxes shown in Tables 2 and 3 serve to provide a check of the precipitation fields and of the wet removal and off-line chemical mechanisms used in the GCTM. The model seems to reproduce observed wet deposition fluxes over the major mid-latitude source regions, which is a necessary condition if the model is to be used to evaluate the impact of the fossil fuel combustion source on NO_y concentrations at regional and remote locations. It appears that wet deposition fluxes in source regions are somewhat underestimated in the LOWWET simulation. However, a definitive statement to this regard is unjustified given the sparse nature of the observations. It should also be noted that similar observations for dry deposition fluxes in source regions are lacking, and thus the model-calculated dry deposition fluxes cannot be independently verified. Rather, they must be indirectly checked by comparing observed and simulated mixing ratios and deposition fluxes at export sites dominated by fossil fuel combustion emissions.

TABLE 3. Comparison of Simulated Annual HNO_3 Wet Deposition Fluxes With Observations at Various European Locations

Location	HNO_3 Wet Deposition Flux, mmoles m^{-2} yr^{-1}		
	OBS[a]	STDWET[b]	LOWWET[c]
Ludlow, England	22	28	20
Vert-le-Petit, France	36	24	18
Faro, Portugal	3	5	4
Hummelfjell, Norway	46	14	12
Velen, Sweden	19	16	14
Dueselbach, Germany	46	49	34
Montelibretti, Italy	22	25	19
Jergul, Norway	3	3	3
Virolahti, Finland	16	13	11
Jarczew, Poland	30	29	23
Semenic, Romania	13	16	14

[a]Observed annual HNO_3 wet deposition flux [*Schaug et al.*, 1987].
[b]Simulated annual HNO_3 wet deposition flux from the STDWET experiment.
[c]Simulated annual HNO_3 wet deposition flux from the LOWWET experiment.

TABLE 4. Comparison of Simulated Annual Mean HNO_3 Surface Mixing Ratios and Wet Deposition Fluxes With Observations in the North Atlantic Basin

Location	Surface HNO_3 Mixing Ratio, pptv		
	OBS[a]	STDWET[b]	LOWWET[c]
Bermuda[d]	370	216–288	325–420
Mace Head, Ireland[d]	280	174–392	258–516
Barbados	190	19	32
	HNO_3 Wet Deposition Flux, mmoles m^{-2} yr^{-1}		
Location	OBS	STDWET	LOWWET
Nova Scotia	16	18	16
Bay de Espoir, Newfoundland	9	11	10
Bermuda[d]	7	5.3–7.2	5.9–7.8
Mace Head, Ireland[d]	5	4.0–6.6	4.0–5.9
Barbados	3	0.3	0.3

[a]Observed annual mean soluble reactive nitrogen mixing ratio [Savoie et al., 1989; also D. L. Savoie et al., unpublished manuscript, 1992].
[b]Model results from the STDWET experiment.
[c]Model results from the LOWWET experiment.
[d]Because of a steep gradient, model results are shown from the box containing the site, as well as from a box to the west.
[e]Observed annual HNO_3 wet deposition flux [Vet et al., 1986; also J. N. Galloway, private communication, 1992].

4.3. *Wet Deposition and Surface Concentrations Over the North Atlantic Basin*

The North Atlantic basin, bounded by the North and Central American, European, and African continents, is thought to be significantly impacted by transport of fossil fuel combustion emissions of sulfur and nitrogen compounds from both the North American and European continents (D. L. Savoie, R. Arimoto, J. M. Prospero, R. A. Duce, W. C. Granstein, K. K. Turekian, J. N. Galloway, and W. C. Keene, Oceanic and anthropogenic contributions to non-sea salt sulfate in the marine boundary layer over the North Atlantic Ocean, submitted to the *Journal of Geophysics*, 1992) (hereinafter referred to as D. L. Savoie et al., submitted manuscript, 1992). In this section, we attempt to quantify the magnitude of this impact by comparing model-calculated wet deposition fluxes and surface concentrations of soluble inorganic nitrogen with observations at representative sites in the North Atlantic basin. Observations of surface concentrations of soluble nitrogen are available for Bermuda, Barbados, and Mace Head, Ireland [*Savoie et al.*, 1989; also D. L. Savoie et al., submitted manuscript, 1992; J. N. Galloway, private communication, 1992]. Wet deposition flux data at these sites are supplemented by data from Nova Scotia and Bay de Espoir, Newfoundland [*Vet et al.*, 1986].

Table 4 shows comparisons of annual mean, model-calculated soluble nitrogen surface concentrations and wet deposition fluxes with observations. The model results ex-

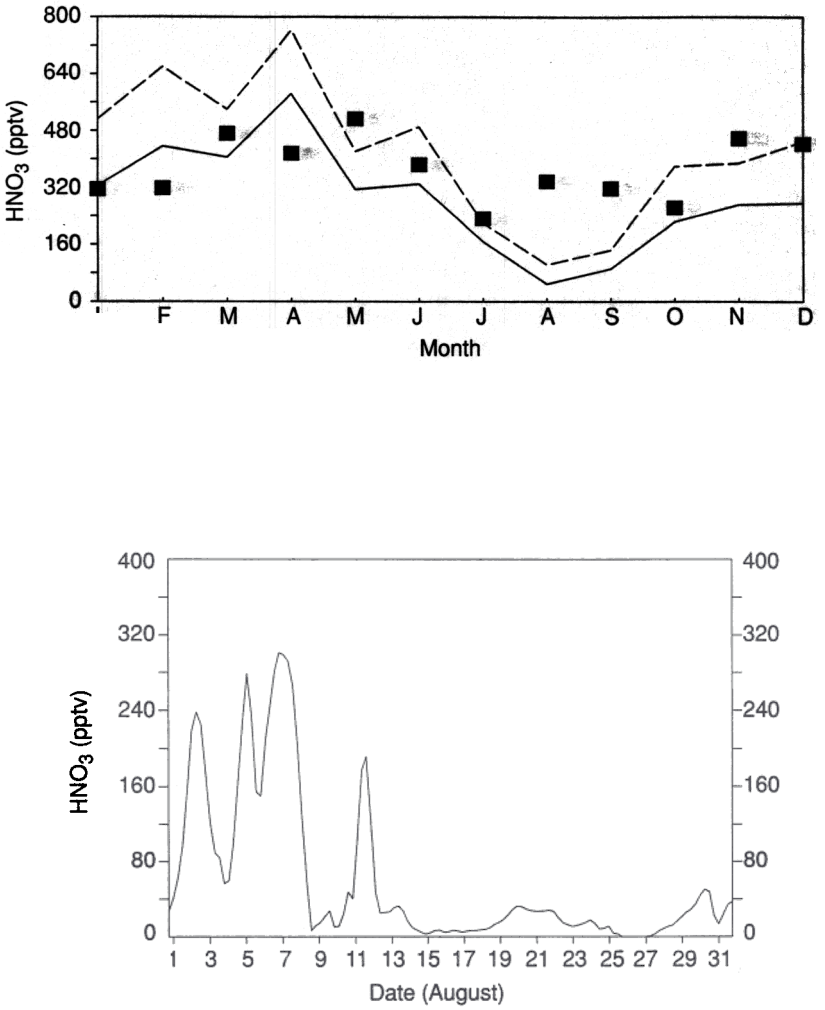

Fig. 6. Modeled and observed variation of surface HNO_3 at Bermuda. Top panel shows monthly mean observations (solid squares), STDWET experiment results (solid line), and LOWWET experiment results (dashed line). Bottom panel shows the simulated time series of HNO_3 at the 990-mbar model level during August from the STDWET experiment.

hibit relatively steep gradients near Bermuda, and therefore values from both the model box containing the station, as well as from a box to the west (~265 km away) are presented. Similarly, simulated tracer gradients are large near Mace Head, Ireland, which is located at the western boundary of the European source region, and hence we present model results from the grid box containing Mace Head, as well as from a box to the west. Both STDWET and LOWWET wet deposition fluxes are in good agreement with measurements at Nova Scotia and Newfoundland, where the NO_y budget may be expected to be dominated by North American emissions. While there is insufficient evidence to say whether one simulation is significantly better than the other, it appears that regional export of fossil fuel combustion emissions from the eastern portion of the North American source region is being well simulated.

At Bermuda, annual-average surface HNO_3 mixing ratios from the LOWWET experiment are in good agreement with observations, while the STDWET mixing ratios account for 60–80% of the observed concentrations. It also appears that the STDWET model slightly overestimates wet deposition near Bermuda, which may be partly due to an excess amount of precipitation in this region of the model. The seasonal variation of modeled and measured surface HNO_3 at Bermuda are shown in Figure 6, along with the simulated time series of STDWET HNO_3 mixing ratios at the 990 mbar model level at this site during August. The LOWWET simulation appears to overestimate winter and spring time mixing ratios but is in better agreement with the fall measurements. Both simulations, however, substantially underestimate summer time surface HNO_3 mixing ratios. Thus the good agreement between the LOWWET model results and annual-average HNO_3 measurements may be fortuitous. On the basis of the STDWET results, we suggest that the fossil fuel source accounts for 60–80% of the observed yearly HNO_3 at Bermuda, with other sources contributing during summer. The simulated August time series (bottom panel of Figure 6) reveals that the underestimate at Bermuda in summer is not due to a lack of transport from North America. During the first part of the month, there are several episodes of elevated HNO_3, while mixing ratios are uniformly low during the latter half of the month. Trajectory analysis based on model winds suggests that episodes of elevated HNO_3 are characterized by transport from North

America, while low mixing ratios are associated with transport from the east and south-east around the Bermuda high. This episodic pattern is also consistent with the observed time series of O_3 at Bermuda [*Oltmans and Levy*, 1992]. By performing separate calculations in which all combustion sources except those in North and South America are turned off, we find that 95% of the surface fossil fuel HNO_3 at Bermuda is from North America at all times of the year.

While the model results at Mace Head bracket the observations, caution should be exercised in interpreting these results as a validation of the long-range transport in the model. We find that the North American source contributes 60–80% of the observed surface HNO_3 at Mace Head during winter but less than 5% during other times of the year. From a model validation standpoint, it would be extremely useful if measurements of other tracers could be used in conjunction with HNO_3 measurements to identify periods during which Mace Head is being impacted by North American emissions.

A very different picture unfolds at Barbados in the tropical Atlantic. At this site the fossil fuel source appears to account for only about 10–15% of the observed surface concentration and wet deposition flux of soluble reactive nitrogen. This region of the Atlantic thus seems to be insulated from the major anthropogenic fossil fuel source regions. However, one can speculate that this is due to a defect in the GCTM. Transport of fossil fuel combustion emissions to Barbados occurs along an anticyclonic sinking path from the mid-latitudes to the tropical east Atlantic, followed by transport in the marine boundary layer. The marine boundary layer of the tropics is characterized by a trade wind inversion which is difficult to resolve in the parent GCM due to inadequate vertical resolution. This could result in the modeled HNO_3 being rapidly mixed to the surface in the east Atlantic, while this mixing may not occur as rapidly in the real world. Thus the model's estimate of dry deposition in the tropical and subtropical oceans may be too high. It should be noted, however, that the extent of mixing that occurs between the maritime inversion layer and the overlying free atmosphere is still a matter of debate. While a detailed study of the effect of the trade wind inversion is beyond the scope of this paper, we have performed a simple test to investigate the potential importance of this effect by repeating the LOWWET experiment with the HNO_3 dry deposition velocity set to 0 over oceans between 25°S and 25°N (we refer to this as the LOWDRY simulation). This results in an annual average HNO_3 surface mixing ratio at Barbados of ~84 pptv, between 50 and 75% of which is from the North American source. Thus it is possible that the tropical North Atlantic is significantly impacted by the anthropogenic fossil fuel source. It should be noted, however, that *Savoie et al.* [1992] concluded that the North American source has little impact on surface HNO_3 at Barbados during winter and spring. Their conclusion was based on isentropic back trajectory analysis, in conjunction with concurrent observations of O_3, NO_3^-, ^{210}Pb, ^7Be, and mineral dust at Barbados. While there is a clear discrepancy between these observations and our model result, further investigation is required to determine whether this is simply due to a lack of interannual variability in the model wind fields, or whether transport from Europe to the tropical North Atlantic is not being adequately simulated in the model.

TABLE 5. Comparison of Simulated Annual Mean Surface HNO_3 Mixing Ratios With Observations in the North Pacific[a]

Location	Surface HNO_3 Mixing Ratio, pptv			
	OBS[b]	STDWET[c]	LOWWET[d]	LOWDRY[e]
Shemya, 53°N, 174°E	94	22	41	41
Midway, 28°N, 177°W	104	46	63	67
Oahu, 21°N, 158°W	130	33	49	97
Enewetak, 11°N, 162°E	56	12	20	46

[a]Observations are soluble reactive nitrogen measuements, while model results are for surface HNO_3.
[b]Observed annual mean soluble reactive nitrogen mixing ratio [*Prospero and Savoie*, 1989].
[c]Model results from the STDWET experiment.
[d]Model results from the LOWWET experiment.
[e]Model results from the LOWDRY experiment.

4.4. *Surface Concentrations Over the North Pacific*

The North Pacific ocean is impacted by emissions from both the Asian and the North American source regions. Transport from the Asian source region peaks during winter and spring, a fact borne out by the spring maximum in dust concentrations observed in the central Pacific [*Uematsu et al.*, 1983]. By contrast, westward transport from the North American source region is associated with the northerly movement of the time mean Pacific subtropical high during summer [*Levy and Moxim*, 1989*a*]. The transport characteristics of the model in this region are described in detail by *Levy and Moxim* [1989*b*] and *Moxim* [1990].

Multiple year surface observations of soluble reactive nitrogen from a string of stations running from Norfolk Island in the central South Pacific to Shemya in the North Pacific [*Prospero and Savoie*, 1989] provide an excellent data base against which the relative impact of various sources of NO_y on this region may be evaluated. In this section we restrict our discussion to the North Pacific stations. The tropical and South Pacific data will be discussed in the next section. Table 5 shows comparisons of model-calculated surface HNO_3 concentrations with measurements of soluble reactive nitrogen at Shemya (53°N, 174°E), Midway (28°N, 177°W), Oahu (21°N, 158°W), and Enewetak (11°N, 162°E).

At Shemya, it is readily evident that only about 25–45% of the observed annual mean soluble nitrogen can be explained in terms of the soluble nitrogen component in the model. This shortfall is difficult to resolve since the stratospheric source has almost no impact at this surface site [*Kasibhatla et al.*, 1991], and the northerly location of this site should preclude a significant impact from the mainly tropical lightning and biomass burning sources. The shortfall in model-calculated surface HNO_3 at Shemya clearly warrants further investigation.

At Midway, the model results indicate that fossil fuel combustion emissions account for about 45–65% of the observed soluble reactive nitrogen. The observations at Oahu might be influenced to some extent by a local source (even though the measurements were only taken during periods of on-shore winds), whereas in our simulations the Hawaiian source has been turned off. It may be noted that the soluble nitrogen shortfall at the Midway, Oahu, and Enewetak sites is approximately 40–100 pptv in the STD-

TABLE 6. Comparison of Simulated NO_x, HNO_3, PAN, and NO_y With Marine Free Tropospheric Measurements Over the Eastern North Pacific

	NASA GTE/CITE 2 Mixing Ratios, pptv[a]			
	NO_x	HNO_3	PAN	NO_y
OBS[b]			120	
STDWET[c]			27–34	
LOWWET[d]			29–37	
	MLOPEX Mixing Ratios, pptv[e]			
	NO_x	HNO_3	PAN	NO_y
OBS[f]				
STDWET[c]				
LOWWET[d]				

[a]Measurements are reported as median values from the CITE 2 experiment conducted in August 1986. Model results represent the range of the August mean 500-mbar mixing ratios from five boxes located between 32°N and 42°N along the 135°W meridian.

[b]NO_x, HNO_3, PAN, and NO_y mixing ratios represent approximate median values for the marine free troposphere [*Carroll et al.*, 1990; *Singh et al.*, 1990; *LeBel et al.*, 1990; *Hübler et al.*, 1992*a*].

[c]Model results from the STDWET experiment.

[d]Model results from the LOWWET experiment.

[e]Measurements are reported as mean values from downslope flow conditions during the MLOPEX experiment at Mauna Loa, Hawaii, in May 1988 [from *Atlas et al.*, 1992, Table 4]. For a list of participants and measurements, refer to *Ridley and Robinson* [1992, Table 1]. Model results represent May mean 685-mbar mixing ratios.

[f]HNO_3 represents sum of HNO_3 and NO_3^-, while PAN represents sum of PAN, $MeONO_2$, and $RONO_2$.

WET and LOWWET simulations. When the HNO_3 dry deposition velocity is set to 0 over the tropical and subtropical oceans (see discussion in section 4.3), the model reproduces 75–80% of the observed surface mixing ratios at Oahu and Enewetak, again suggesting that one possible explanation for the shortfall in model estimates may be an overestimation of dry deposition over the tropical and subtropical oceans. All three of these sites may also be expected to be influenced by the tropical lightning source. However, the extent to which this source can account for the HNO_3 shortfall in the model remains to be quantified.

4.5. *Marine Free Tropospheric Concentrations Over the North Pacific*

Mid-tropospheric measurements of NO_y made over the eastern North Pacific between 30° and 45°N made during August 1986, as part of the NASA GTE/CITE 2 experiment [*Carroll et al.*, 1990; *LeBel et al.*, 1990; *Singh et al.*, 1990; *Hübler et al.*, 1992*a*] provide another useful data base against which the model results may be compared. For the sake of comparison, we will discuss our results in terms of the August mean 500 mbar model mixing ratios from five representative boxes located between 32°N and 42°N along the 130°W meridian. These comparisons are presented in Table 6.

Both the STDWET and LOWWET simulations suggest that the fossil fuel source only accounts for 15–25% of the observed NO_x, while half to essentially all of the measured HNO_3 appears to be due to the fossil fuel source. While the stratospheric source does not significantly impact NO_x (about 3 pptv) and PAN (about 7 pptv) levels in this region at 500 mbar, it does contribute about 25 pptv of HNO_3 [*Kasibhatla et al.*, 1991]. However, in the context of comparing observed and model mixing ratios of individual NO_y components, it is also important to characterize that fraction of the observed NO_y that cannot be explained in terms of the measured NO_x, HNO_3, and PAN. Thus for the purposes of this study, it is probably more appropriate to compare simulated NO_y levels against observations. NO_y mixing ratios ranging from ~100 pptv to greater than 1 ppbv, with a median of ~300 pptv, were observed at altitudes of 4.6–5.0 km [*Ridley et al.*, 1990; *Ridley*, 1991]. Model-simulated NO_y mixing ratios range from 74–110 pptv to 101–170 pptv for the STDWET and LOWWET scenarios, respectively, leaving a shortfall of 125–225 pptv to be explained by other sources. Of this, approximately 35 pptv can be explained by downward transport from the stratosphere. However, another important point should not be overlooked. It is likely that some of the maritime measurements may be influenced to some extent by the proximity of the measurement region to the California coast. To illustrate our point, consider flight 7 of the CITE 2 mission. During this flight, mid-tropospheric NO_y levels, as well as mixing ratios of tracers such as CO, were significantly lower than those observed during other maritime flights, and it appeared that air with a long marine residence time was being sampled [*Singh et al.*, 1990]. The median NO_y mixing ratio observed during this flight was 150 pptv [*Ridley et al.*, 1990]. When the LOWWET simulation is repeated with the North American fossil fuel source turned off, simulated mid-tropospheric NO_y mixing ratios range from 60–130 pptv. Taking into account the contribution from the stratospheric source, we find that these two sources can then explain most of the mid-tropospheric NO_y measured during this flight. Thus part of the model shortfall when all maritime CITE 2 data are considered may be due an inadequate resolution of subgrid scale transport from adjacent continental source regions in the model and does not necessarily indicate that other sources contribute significantly to the NO_y budget of this region.

Extensive measurements of NO_y and its constituents were also carried out at Mauna Loa, Hawaii, during the month-long MLOPEX experiment in May 1988 [*Ridley and Robinson*, 1992]. The measurement site is located at an altitude of 3.4 km, and it has been argued that measured mixing ratios during downslope flow are representative of marine free tropospheric mixing ratios in this region [*Walega et al.*, 1992; *Hübler et al.*, 1992*b*; *Atlas et al.*, 1992]. At this point it should be noted that there appears to be a slight discrepancy in the literature regarding the downslope flow criterion for defining free tropospheric air sampling periods. *Greenberg et al.* [1992] found that ethylene and propylene were present in air sampled during most downslope flow periods. They suggest that the presence of these species may be the result of recent transport from sources at the surface and speculate that island effects may be the mechanism responsible for this transport. If this is indeed the case, then it raises the question as to whether the downslope NO_y measurements at Mauna Loa could also be affected by island sources or by mixing of air from the marine boundary layer around the island.

Measurements (taken from *Atlas et al.* [1992, Table 4]) filtered so as to include only the downslope values are compared to model-calculated 685 mbar mixing ratios during May in Table 6. Again, caution should be exercised in

comparing model-calculated mixing ratios of individual components against observations, given the fact the "missing" NO_y fraction comprises about 25% of the total measured NO_y. Our model results suggest that only 15–30% of the NO_y observed during downslope flow conditions at Mauna Loa can be attributed to long-range transport from continental fossil fuel source regions. This conclusion is in accord with the analysis by *Hübler et al.* [1992*b*], who found that there was no correlation between NO_y and tracers of anthropogenic sources during downslope flow conditions. They therefore suggest that much of this NO_y has a stratospheric and/or upper tropospheric origin. Our earlier calculations indicate that the stratospheric source only contributes about 25 pptv of NO_y during this time of the year [*Kasibhatla et al.*, 1991], suggesting that the upper tropospheric lightning source may be contributing significantly to the free tropospheric NO_y budget in this region.

To address the question raised earlier regarding the possibility of mixing air from the marine boundary layer, we examine 940-mbar model results from the LOWDRY experiment. This experiment is chosen since it represents our upper limit calculation of the impact of fossil fuel combustion on NO_y at Mauna Loa. The mean 940-mbar NO_y mixing ratio from this experiment is 130 pptv, which still accounts for only half of the measured NO_y. Note, however, that this only represents fossil fuel NO_y from continental sources, since in our model simulations the Hawaiian source has been turned off.

4.6. *Impact of Fossil Fuel Combustion Emissions on the Remote Troposphere*

It is important to assess the anthropogenic influence on the remote tropospheric NO_y budget in order to make progress in obtaining a quantitative understanding of the influence of humans on the global tropospheric O_3 budget. Observations of surface nitrate at island stations in the central equatorial and southern Pacific provide a hint of background levels of reactive nitrogen in the remote troposphere. Such a set of observations is available at seven stations: Fanning (4°N, 159°W), Nauru (1°S, 167°E), Funafuti (8°S, 179°E), Samoa (14°S, 171°W), Rarotonga (21°S, 160°W), New Caledonia (22°S, 166°E), and Norfolk Island (29°S, 169°E), which are part of the SEAREX network [*Prospero and Savoie*, 1989]. Comparisons of model-calculated, annual mean surface nitrate concentrations with corresponding multiyear measurements of soluble nitrogen at these stations are shown in Table 7. We find it extremely significant that the fossil fuel combustion source only contributes 1–5 pptv of HNO_3 at these sites, except at New Caledonia and Norfolk Island which are affected by regional sources in Australia. At all sites, the shortfall in model-calculated surface HNO_3 is of the order of 40–50 pptv. This is roughly the same order of magnitude as the shortfall at Midway, Oahu, and Enewetak (see discussion in section 4.4). An even stronger argument for the minimal impact of the fossil fuel source at the remote South Pacific tropical sites can be made by considering results from the LOWDRY simulation, in which the HNO_3 dry deposition velocity set to 0 over the tropical and subtropical oceans. Simulated annual average surface HNO_3 mixing ratios in this experiment range from 6–9 pptv, leaving a shortfall of about 30–50 pptv. *Penner et al.* [1991] concluded that the natural NO_x sources, including a 3 Tg N yr^{-1} lightning source, cannot account for the observed surface HNO_3 mixing ratios in the remote Pacific. *Kasibhatla et al.* [1991] have confirmed that the stratospheric source has a negligible impact on surface HNO_3 in this region, and our preliminary calculations suggest that the transport of biomass burning emissions also has only a small impact in this region. We are therefore left with two possibilities: (1) that the magnitude of the lightning source is such that the resulting surface HNO_3 concentrations over the remote equatorial and tropical Pacific are of the order of 30–50 pptv; the other possibility is that some other source, as yet unknown, is responsible for the observed background surface HNO_3 concentrations at these sites. A similar conclusion has been reached by *Penner et al.* [1991].

TABLE 7. Comparison of Simulated Annual Mean Surface HNO_3 Mixing Ratios With Observations in the Tropical and South Pacific[a]

Location	Surface HNO_3 Mixing Ratio, pptv			
	OBS[b]	STDWET[c]	LOWWET[d]	LOWDRY[e]
Fanning, 4°N, 159°W	59	2	5	9
Nauru, 1°S, 167°E	59		3	6
Funafuti, 8°S, 179°E	39	1	3	7
Samoa, 14°S, 171°W	40	2	3	6
Rarotonga, 21°S, 160°W	42	2	3	6
New Caledonia, 22°S, 166°E	76	29	34	59
Norfolk Island, 29°S, 169°E	66	12	17	

[a]Observations are soluble reactive nitrogen measurements, while model results are for surface HNO_3.
[b]Observed annual mean of soluble reactive nitrogen mixing ratio [*Prospero and Savoie*, 1989].
[c]Model results from the STDWET experiment.
[d]Model results from the LOWWET experiment.
[e]Model results from the LOWDRY experiment.

Levy and Moxim [1989*a*] concluded that transport of fossil fuel combustion emissions from the NH is not significant in terms of SH NO_y levels due to efficient wet removal at the Inter-Tropical Convergence Zone. We reexamine this issue in the light of the current multiple-species formulation which explicitly treats PAN as a transported species. Observed wet deposition fluxes, which provide a hint of total NO_y levels, range from 2–4 mMoles N m^{-2} yr^{-1} at Katherine, Australia and Amsterdam Island, two remote sites in the southern hemisphere [*Galloway et al.*, 1982]. We find that only 5–10% of these fluxes are due to long-range transport and subsequent deposition of fossil fuel combustion emissions. Again, it remains to be seen whether the other known NO_x sources can explain these observations.

While mid- and upper tropospheric measurements in the remote troposphere are generally lacking, NO_y measurements over Darwin, Australia (12°S, 131°E), and Guam (14°N, 145°E), which were made as part of the tropical Stratosphere-Troposphere Exchange Program (STEP) during January and February 1987 provide a hint of the levels of NO_y occurring in these regions. The average observed NO_y mixing ratio during the STEP experiment was approximately 400 pptv between the 190- and 315-mbar model levels [*Murphy et al.*, 1992]. Our calculations indicate that the fossil fuel source only contributes an average of about 10–30 pptv of NO_y at these altitudes during January and February,

which is of the same magnitude as the NO_y levels produced by the stratospheric source [*Kasibhatla et al.*, 1991]. Since this region of the tropics is one of high convective activity, it is likely that production of NO_x by lightning is the dominant source of mid- and upper tropospheric NO_y in this part of the world [*Murphy et al.*, 1992].

4.7. *Impact of Fossil Fuel Combustion Emissions on the High Northern Latitudes*

It has been speculated that transport of anthropogenically produced NO_y could be influencing O_3 photochemistry in the high northern latitudes [*Jacob et al.*, 1992; *Singh et al.*, 1992]. This hypothesis is based on an analysis of trace gas measurements from the ABLE 3A study over western Alaska during the summer of 1988. In this section we attempt to quantify the impact of long-range transport of fossil fuel combustion emissions on the NO_y budget of the high northern latitudes during summer by comparing model calculations with the ABLE 3A measurements, as well as with a few measurements in this region during other times of the year.

Mean NO_y mixing ratios measured during the ABLE 3A experiment range from 370 pptv in the boundary layer, to approximately 700 pptv in the free troposphere [*Sandholm et al.*, 1992]. Our model results suggest that the fossil fuel combustion source contributes at most 35% of the total NO_y in the free troposphere, and even less at lower altitudes, during summer between 60°N and 70°N in western Alaska. Model-calculated fossil fuel NO_y deposition (wet + dry) during this time of the year is $0.75–1.15 \times 10^9$ molecules $cm^{-2}\ s^{-1}$, compared to the observed mean deposition flux of 5.6×10^9 molecules $cm^{-2}\ yr^{-1}$ [*Talbot et al.*, 1992; *Bakwin et al.*, 1992], again suggesting that long-range transport of fossil fuel combustion emissions has a small impact on the summer time NO_y budget of this region. Our previous simulations with the stratospheric source indicate that this source contributes about 60–80 pptv of NO_y during summer in the free troposphere, but only negligibly small amounts in the high northern latitude lower troposphere. Also, the total deposition from this source is less than 0.2×10^9 molecules $cm^{-2}\ s^{-1}$ in this region.

Thus our conclusion regarding the impact of the fossil fuel source seems to be in accord with that by *Wofsy et al.* [1992]. However, our model results provide for only a small contribution to the deposition flux from the stratospheric source, while *Wofsy et al.* [1992] argue that this source is important at high northern latitudes. *Jacob et al.* [1992] argue that biomass burning emissions probably contribute only about 20% of the NO_y in this region during summer, and *Bakwin et al.* [1992] estimate that emissions from soils are quite small (0.13×10^9 molecules $cm^2\ s^{-1}$). Thus there appears to be a significant gap between the observed and modeled summer time NO_y budget in high northern latitudes. One possibility that cannot be ruled out is that the fossil fuel source strength in Siberia and Russia has been underestimated in this study. Another possibility is that emissions from aircraft contribute significant quantities of NO_y at high northern latitudes. We note, however, that the model-calculated surface mixing ratios (~500 pptv) are in relatively good agreement with measured background concentrations of NO_y at Barrow, Alaska, during spring [*Jaffe et al.*, 1991], as well as with year round PAN measurements at Alert in the Canadian Arctic (82°N, 62°W) [*Barrie and Bottenheim*, 1991]. Clearly, further investigation (measurements as well as model studies) is required to unravel the contributions of various sources to the NO_y budget at high northern latitudes.

5. SUMMARY

Detailed comparisons of simulated NO_x, HNO_3, and PAN distributions from fossil fuel combustion emissions with observations at various locations have been presented in an attempt to quantify the impact of this source on tropospheric NO_y levels. Our calculations clearly demonstrate the need to explicitly treat PAN as a transported species, and we find that PAN is the dominant component of fossil fuel NO_y away from source regions poleward of 45°N. Simulated wet deposition fluxes over the North American and European source regions are in good agreement with observations. We find that the export of fossil fuel combustion emissions is sufficient to explain a significant fraction of the observed surface nitrate concentrations and wet deposition fluxes in the extratropical North Atlantic basin, with other sources probably having some impact during summer. The fact that wet deposition in source regions and wet deposition and surface mixing ratios at Bermuda are well simulated, supports the model prediction that dry deposition is a major sink of fossil fuel NO_y in source regions. Only a small fraction of the surface nitrate at Barbados in the tropical North Atlantic appears to be due to the fossil fuel source. However, a possible defect in the GCTM related to an inadequate simulation of the trade wind inversion in the parent GCM cannot be ruled out, and our upper-limit calculations indicate that almost half the observed surface HNO_3 in this region of the Atlantic may be due to long-range transport from the fossil fuel combustion source regions. We also find that the fossil fuel source, along with some contribution from the stratospheric source, can explain between half and two thirds of the summer time NO_y measurements in the marine free troposphere of the eastern Pacific. While this may indicate that other sources impact the NO_y budget in this region, one cannot rule out the possibility that the model does not adequately resolve subgrid-scale transport from continental source regions adjacent to the experimental region. At the more remote Mauna Loa site, we find that distant fossil fuel sources can account for less than 30% of the observed soluble reactive nitrogen concentrations. Our calculations indicate that the fossil fuel source has only a minor impact on surface nitrate concentrations in the remote tropical Pacific, as well as on deposition fluxes in the remote SH. In the high northern latitudes, we find that less than a third of the observed summer time mid- and lower tropospheric NO_y levels can be explained in terms of long-range transport from the fossil fuel combustion source regions.

Acknowledgments. This work was supported in part by funds from the National Science Foundation under grant ATM-8905901. We wish to thank E. L. Atlas, M. P. Buhr, J. N. Galloway, D. M. Murphy, J. M. Prospero, S. T. Sandholm, D. L. Savoie, and H. B. Singh for providing data prior to publication, and M. Kanakidou for providing ethane and propane fields from her model simulations. We also wish to acknowledge comments on the original version of this paper by E. L. Atlas, A. J. Broccoli, W. L. Chameides, J. D. Mahlman, and by two anonymous reviewers.

REFERENCES

Atkinson, R., and A. C. Lloyd, Evaluation of kinetic and mechanistic data for modeling of photochemical smog, *J. Phys. Chem. Ref. Data*, *13*, 315–440, 1984.

Atlas, E. L., B. A. Ridley, G. Hübler, J. G. Walega, M. A. Carroll, D. D. Montzka, B. J. Huebert, R. B. Norton, F. E. Grahek, and S. Schauffler, Partitioning and budget of NO_y species during the Mauna Loa Photochemistry Experiment, *J. Geophys. Res.*, *97*, 10,449–10,462, 1992.

Bakwin, P. S., S. C. Wofsy, S.-M. Fan, and D. R. Fitzjarrald, Measurements of NO_x and NO_y concentrations and fluxes over Arctic tundra, *J. Geophys. Res.*, *97*, 16,545–16,557, 1992.

Barrie, L. A., and J. W. Bottenheim, Sulfur and nitrogen pollution in the Arctic atmosphere, in *Pollution of the Arctic Atmosphere*, edited by W. T. Sturges, pp. 155–183, Elsevier Science, New York, 1991.

Beck, J. P., C. E. Reeves, F. A. A. M. de Leeuw, and S. A. Penkett, The effect of aircraft emissions on tropospheric ozone in the northern hemisphere, *Atmos. Environ.*, *26A*, 17–29, 1992.

Cadle, S. H., J. M. Dasch, and P. A. Mulawa, Atmospheric concentrations and the deposition velocity to snow of nitric acid, sulfur dioxide and various particulate species, *Atmos. Environ.*, *19*, 1819–1827, 1985.

Carroll, M. A., et al., Aircraft measurements of NO_x over the eastern Pacific and continental United States and implications for ozone production, *J. Geophys. Res.*, *95*, 10,205–10,233, 1990.

Chameides, W. L., and A. Tan, The two-dimensional diagnostic model for tropospheric OH: An uncertainty analysis, *J. Geophys. Res.*, *86*, 5209–5223, 1981.

Chameides, W. L., et al., Ozone precursor relationships in the ambient atmosphere, *J. Geophys. Res.*, *97*, 6037–6055, 1992.

Crutzen, P. J., Photochemical reaction initiated by and influencing ozone in unpolluted tropospheric air, *Tellus*, *26*, 45–55, 1974.

Dana, M. T., and R. C. Easter, Statistical summary and analyses of event precipitation chemistry from the MAP3S network, 1976–1983, *Atmos. Environ.*, *21*, 113–128, 1987.

DeMore, W. B., J. J. Margitan, M. J. Molina, R. T. Watson, D. M. Golden, R. F. Hampson, M. J. Kurylo, C. J. Howard, and A. R. Ravishankara, Chemical kinetics and photochemical data for use in stratospheric modeling, Evaluation number 9, NASA, *JPL Publ. 90-1*, 217 pp., Pasadena, Calif., 1990.

Galloway, J. N., G. E. Likens, W. C. Keene, and J. M. Miller, The composition of precipitation in remote areas of the world, *J. Geophys. Res.*, *87*, 8771–8786, 1982.

Galloway, J. N., Z. Dianwu, X. Jiling, and G. E. Likens, Acid rain: China, United States, and a remote area, *Science*, *236*, 1559–1562, 1987.

Giorgi, F., and W. L. Chameides, Rainout lifetimes of highly soluble aerosols and gases as inferred from simulations with a general circulation model, *J. Geophys. Res.*, *91*, 14,367–14,376, 1986.

Greenberg, J. P., P. R. Zimmerman, W. F. Pollock, R. A. Lueb, and L. E. Heidt, Diurnal variability of atmospheric methane, nonmethane hydrocarbons, and carbon monoxide at Mauna Loa, *J. Geophys. Res.*, *97*, 10,395–10,413, 1992.

Hameed, S., and J. Dignon, Changes in the geographical distributions of global emissions of NO_x and SO_x from fossil fuel combustion between 1966 and 1980, *Atmos. Environ.*, *22*, 441–449, 1988.

Hübler, G., D. W. Fahey, B. A. Ridley, G. L. Gregory, and F. C. Fehsenfeld, Airborne measurements of total reactive odd nitrogen (NO_y), *J. Geophys. Res.*, *97*, 9833–9850, 1992*a*.

Hübler, G., et al., Total reactive oxidized nitrogen (NO_y) in the remote Pacific troposphere and its correlation with O_3 and CO: Mauna Loa Photochemistry Experiment 1988, *J. Geophys. Res.*, *97*, 10,427–10,447, 1992*b*.

Huebert, B. J., and C. H. Robert, The dry deposition of nitric acid to grass, *J. Geophys. Res.*, *90*, 2085–2090, 1985.

Jacob, D. J., et al., Summertime photochemistry of the troposphere at high northern latitudes, *J. Geophys. Res.*, *97*, 16,421–16,431, 1992.

Jaffe, D. A., R. E. Honrath, J. A. Herring, S.-M. Li, and J. D. Kahl, Measurements of nitrogen oxides at Barrow, Alaska during spring: Evidence for regional and Northern Hemisphere sources of pollution, *J. Geophys. Res.*, *96*, 7395–7405, 1991.

Kanakidou, M., H. B. Singh, K. M. Valentin, and P. J. Crutzen, A two-dimensional study of ethane and propane oxidation in the troposphere, *J. Geophys. Res.*, *96*, 15,395–15,413, 1991.

Kasibhatla, P. S., H. Levy, II, W. J. Moxim, and W. L. Chameides, The relative impact of stratospheric photochemical production on tropospheric NO_y levels: A model study, *J. Geophys. Res.*, *96*, 18,631–18,646, 1991.

LeBel, P. J., B. J. Huebert, H. I. Schiff, S. A. Vay, S. E. VanBramer, and D. R. Hastie, Measurements of tropospheric nitric acid over the western United States and northeastern Pacific Ocean, *J. Geophys. Res.*, *95*, 10,199–10,204, 1990.

Levy, II, H., Normal atmosphere: Large radical and formaldehyde concentrations predicted, *Science*, *173*, 141–143, 1971.

Levy, II, H., J. D. Mahlman, and W. J. Moxim, Tropospheric N_2O variability, *J. Geophys. Res.*, *87*, 3061–3080, 1982.

Levy, II, H., and W. J. Moxim, Simulated global distribution and deposition of reactive nitrogen emitted by fossil fuel combustion, *Tellus*, *41*, 256–271, 1989*a*.

Levy, II, H., and W. J. Moxim, Influence of long-range transport of combustion emissions on the chemical variability of the background atmosphere, *Nature*, *338*, 326–328, 1989*b*.

Logan, J. A., Nitrogen oxides in the troposphere: Global and regional budgets, *J. Geophys. Res.*, *88*, 10,785–10,807, 1983.

Mahlman, J. D., and W. J. Moxim, Tracer simulation using a global general circulation model: Results from a midlatitude instantaneous source experiment, *J. Atmos. Sci.*, *35*, 1340–1374, 1978.

Manabe, S., and J. L. Holloway, Jr., The seasonal variation of the hydrologic cycle as simulated by a global model of the atmosphere, *J. Geophys. Res.*, *80*, 1617–1649, 1975.

Manabe, S., D. G. Hahn, and J. L. Holloway, Jr., The seasonal variation of the tropical circulation as simulated by a global model of the atmosphere, *J. Atmos. Sci.*, *31*, 43–83, 1974.

Moxim, W. J., Simulated transport of NO_y to Hawaii during August: A synoptic study, *J. Geophys. Res.*, *95*, 5717–5729, 1990.

Murphy, D. M., D. W. Fahey, S. C. Liu, M. H. Proffitt, and C. S. Eubank, Reactive nitrogen and its correlation with ozone in the lower stratosphere and upper troposphere, *J. Geophys. Res.*, in press, 1992.

Oltmans, S. J., and H. Levy, II, Seasonal cycle of surface ozone over the western North Atlantic, *Nature*, *358*, 392–395, 1992.

Penner, J. E., C. S. Atherton, J. Dignon, S. J. Ghan, J. J. Walton, and S. Hameed, Tropospheric nitrogen: A three-dimensional study of sources, distributions, and deposition, *J. Geophys. Res.*, *96*, 959–990, 1991.

Prospero, J. M., and D. L. Savoie, Effect of continental sources on nitrate concentrations over the Pacific Ocean, *Nature*, *339*, 687–689, 1989.

Prospero, J. M., J. Galloway, R. Wollast, and D. L. Savoie, The atmospheric deposition of nutrient-nitrogen to the world ocean (GESAMP) paper presented at AMS Symposium on the Role of Oceans as a Source and Sink of Trace Substances that Influence Global Change, Anaheim, Calif., February 1990.

Ridley, B. A., Recent measurements of oxidized nitrogen compounds in the troposphere, *Atmos. Environ.*, *25A*, 1905–1926, 1991.

Ridley, B. A., and E. Robinson, The Mauna Loa Photochemistry Experiment, *J. Geophys. Res.*, *97*, 10,285–10,290, 1992.

Ridley, B. A., et al., Ratios of peroxyacetylnitrate to active nitrogen observed during aircraft flight over the eastern Pacific oceans and continental United States, *J. Geophys. Res.*, *95*, 10,179–10,192, 1990.

Sandholm, S. T., et al., Summertime tropospheric observations related to N_xO_y distributions and partitioning over Alaska: Arctic Boundary Layer Expedition 3A, *J. Geophys. Res.*, *97*, 16,481–16,509, 1992.

Savoie, D. L., J. M. Prospero, and E. S. Saltzman, Nonseasalt sulfate and nitrate in tradewind aerosols at Barbados: evidence for long-range transport, *J. Geophys. Res.*, *94*, 5069–5080, 1989.

Savoie, D. L., J. M. Prospero, S. J. Oltmans, W. C. Graustein, K. K. Turekian, J. T. Merrill, and H. Levy II, Sources of nitrate and ozone in the marine boundary layer of the tropical North Atlantic, *J. Geophys. Res.*, *97*, 11,575–11,589, 1992.

Schaug, J., J. E. Hansen, K. Nodop, B. Ottar, and J. M. Pacyna, Summary report from the chemical co-ordinating centre for the third phase of EMEP, Norwegian Institute for Air Research, Lillestrom, Norway, 1987.

Shepson, P. B., K. G. Anlauf, J. W. Bottenheim, H. A. Wiebe, N. Gao, and K. Muthuramu, Distribution of reactive nitrogen at a rural site in Ontario during spring 1990 as part of the Eulerian model evaluation field study (EMEFS), paper presented at CHEMRAWN VII, World Conference on the Chemistry of the

Atmosphere: Its Impact on Global Change, Baltimore, Md., Dec. 2–6, 1991.

Singh, H. B., et al., Peroxyacetyl nitrate measurements during CITE 2: Atmospheric distribution and precursor relationships, *J. Geophys. Res.*, *95*, 10,163–10,178, 1990.

Singh, H. B., D. O'Hara, D. Herlth, J. D. Bradshaw, S. T. Sandholm, G. L. Gregory, G. W. Sachse, D. R. Blake, P. J. Crutzen, and M. A. Kanakidou, Atmospheric measurements of peroxyacetyl nitrate and other organic nitrates at high latitudes: Possible sources and sinks, *J. Geophys. Res.*, *97*, 16,511–16,522, 1992.

Talbot, R. W., A. S. Vijgen, and R. C. Harriss, Soluble species in the Arctic summer troposphere: Acidic gases, aerosols, and precipitation, *J. Geophys. Res.*, *97*, 16,531–16,543, 1992.

Trainer, M., et al., Observations and modeling of the reactive nitrogen photochemistry at a rural site, *J. Geophys. Res.*, *96*, 3045–3063, 1991.

Uematsu, M., R. A. Duce, J. M. Prospero, L. Q. Chen, J. T. Merrill, and R. L. McDonald, The transport of mineral aerosol from Asia over the North Pacific Ocean, *J. Geophys. Res.*, *88*, 5343–5352, 1983.

Vaghjiani, G. L., and A. R. Ravishankara, New measurements of the rate coefficient for the reaction of OH with methane, *Nature*, *350*, 406–409, 1991.

Van Valin, C. C., M. Luria, J. D. Ray, and J. F. Boatman, A comparison of surface and airborne trace gas measurements at a rural Pennsylvania site, *J. Geophys. Res.*, *96*, 20,745–20,754, 1991.

Vet, R. J., W. B. Sukoff, M. E. Still, and R. Gilbert, CAPMoN precipitation chemistry data summary 1983–1984, Atmospheric Environment Service, Downsview, Ontario, 1986.

Voldner, E. C., L. A. Barrie, and A. Sirois, A literature review of dry deposition of oxides of sulfur and nitrogen with emphasis on long-range transport modeling in North America, *Atmos. Environ.*, *20*, 2101–2123, 1986.

Walcek, C. J., R. A. Brost, J. S. Chang, and M. L. Wesely, SO_2, sulfate, and HNO_3 deposition velocities computed using regional land use and meteorological data, *Atmos. Environ.*, *20*, 949–964, 1986.

Walega, J. G., B. A. Ridley, S. Madronich, F. E. Grahek, J. D. Shetter, T. D. Sauvain, C. J. Hahn, J. T. Merill, B. A. Bodhaine, and E. Robinson, Observations of peroxyacetyl nitrate, peroxypropionyl nitrate, methyl nitrate and ozone during the Mauna Loa Observatory Photochemical Experiment, *J. Geophys. Res.*, *97*, 10,311–10,330, 1992.

Wesely, M. L., J. A. Eastman, D. H. Stedman, and E. D. Yalvac, An eddy correlation measurement of NO_2, *Atmos. Environ.*, *16*, 815–820, 1982.

Wofsy, S. C., et al., Atmospheric chemistry in the Arctic and Subarctic: Influence of natural fires, industrial emissions, and stratospheric inputs, *J. Geophys. Res.*, *97*, 16,731–16,746, 1992.

P. Kasibhatla, H. Levy II, and W. J. Moxim, Geophysical Fluid Dynamics Laboratory, Box 308, Princeton University, Princeton, NJ 08542.

(Received February 26, 1992;
revised November 25, 1992;
accepted November 30, 1992.)